

# Electroformation of Giant Phospholipid Vesicles on a Silicon Substrate: Advantages of Controllable Surface Properties

Maël Le Berre,<sup>†</sup> Ayako Yamada,<sup>‡</sup> Lukas Reck,<sup>†</sup> Yong Chen,<sup>†</sup> and Damien Baigl<sup>\*,†</sup>

Department of Chemistry, Ecole Normale Supérieure, Paris F-75005, France, and Department of Physics, Graduate School of Science, Kyoto University, Kyoto 606-8502, Japan

Received November 2, 2007. In Final Form: December 19, 2007

We introduce the use of silicon (Si) as a substrate for the electroformation of giant phospholipid vesicles. By taking advantage of the tunability of silicon surface properties, we varied the organization of the phospholipid film on the electrode and studied the consequences on vesicle formation. In particular, we investigated the effects of Si surface chemistry and microtopology on the organization of the phospholipid film and the properties of the final vesicles. We established correlations between chemical homogeneity, film defects, and resulting vesicle size distribution. By considering phospholipid films that are artificially fragmented by electrode microstructures, we showed that the characteristic size of vesicles decreases with a decrease in microstructure dimensions. We finally proposed a way to control the vesicle size distribution by using a micropatterned silicon dioxide layer on a Si substrate.

## Introduction

Giant phospholipid vesicles (i.e., with a diameter ranging from a few micrometers to a few hundred micrometers) have attracted a growing interest because of their relevance for a number of biological and chemical applications.<sup>1–5</sup> Several techniques for their preparation have been proposed such as spontaneous swelling,<sup>6,7</sup> electroformation,<sup>8–10</sup> microfluidics,<sup>11,12</sup> or droplet transfer.<sup>13</sup> Among them, the electroformation method proposed by Angelova and Dimitrov<sup>8</sup> has been widely used. It consists of applying AC field between two platinum or tin-doped indium oxide (ITO) electrodes coated by a phospholipid film and separated by an aqueous solution. This technique is simple and efficient but does not allow one to achieve precise control of the vesicles' formation, mainly because ITO surface properties and lipid film organization on the surface cannot be easily controlled. In contrast, due to the extensive development of the microelectronics industry, silicon (Si) has become a very well-controlled material.<sup>14</sup> Furthermore, biophysicists have commonly used silicon as a substrate for investigations on supported phospholipid

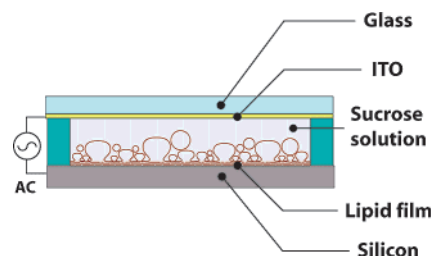


**Figure 1.** Experimental setup for the electroformation on silicon.

membranes.<sup>15–17</sup> In this paper, we introduce the use of a Si substrate with controlled surface properties for the electroformation of giant vesicles. In particular, we investigated the effects of Si surface chemistry and microstructuration on phospholipid film organization and properties of the final vesicles.

## Materials and Methods

**Materials.** [100] boron-doped silicon (Si) wafers (thickness: 500  $\mu\text{m}$  and resistivity: 1–10  $\Omega\text{cm}$ ) were purchased from Siltronic, buffered hydrofluoric acid BOE7:1 was from Technic France, and the AZ5214 photoresist was from Clariant. All other chemicals were from Sigma. Ultrapure water (Millipore, 18 M $\Omega\text{cm}$ ) was used for all experiments.

**Electroformation.** For all experiments, the same electroformation procedure was applied. First, 1.5  $\mu\text{L}$  of a 20 mg/mL egg phosphatidylcholine (EPC) solution containing 4 wt % fluorescein-labeled phosphoethanolamine (PE-FITC) in chloroform/methanol (9:1 vol/vol) was spread at a constant speed with a micropipette tip on the electrode substrate (ITO or Si) previously cleaned by isopropyl alcohol/acetone/sonication. Under these conditions, the film thickness was reproducible for a given substrate according to the film color and ellipsometry measurements. However, the film thickness depended on the nature of the surface (surface chemistry and microstructures). The electrode substrate was separated from the ITO counter-electrode using a 1 mm silicone rubber spacer, which delimited a swelling surface of 1.8  $\text{cm}^2$  (Figure 1). After the phospholipid film was dried under vacuum, a swelling solution

\* Corresponding author. E-mail: damien.baigl@ens.fr; tel.: +33 1 4432 2431; fax: +33 1 4432 2402.

<sup>†</sup> Ecole Normale Supérieure.

<sup>‡</sup> Kyoto University.

(1) Karlsson, A.; Karlsson, R.; Karlsson, M.; Cans, A. S.; Stromberg, A.; Ryttsen, F.; Orwar, O. *Nature (London, U.K.)* **2001**, *409*, 150–152.

(2) Noireaux, V.; Libchaber, A. *Proc. Natl. Acad. Sci. U.S.A.* **2004**, *101*, 17669–17694.

(3) Chen, I. A.; Salehi-Ashtiani, K.; Szostak, J. W. *J. Am. Chem. Soc.* **2005**, *127*, 13213–13219.

(4) Luisi, P. L.; Walde, P. *Giant Liposomes, Perspectives in Supramolecular Chemistry*; John Wiley and Sons Ltd.: New York, 2000.

(5) Lasic, D. D. *Liposomes in Gene Delivery*; CRC Press: Boca Raton, FL, 1987.

(6) Reeves, J. P.; Dowben, R. M. *J. Cell Physiol.* **1969**, *73*, 49–60.

(7) Needham, D.; Evans, E. *Biochemistry* **1988**, *27*, 8261–8269.

(8) Angelova, M. I.; Dimitrov, D. S. *Faraday Discuss. Chem. Soc.* **1986**, *81*, 303–311.

(9) Angelova, M. I.; Soleau, S.; Méléard, P.; Faucon, J.-F.; Bothorel, P. *Prog. Colloid Polym. Sci.* **1992**, *89*, 127–131.

(10) Estes, D. J.; Mayer, M. *Colloids Surf., B* **2005**, *42*, 115–123.

(11) Dittrich, P. S.; Heule, M.; Renaud, P.; Manz, A. *Lab Chip* **2006**, *6*, 488–493.

(12) Funakoshi, K.; Suzuki, H.; Takeuchi, S. *J. Am. Chem. Soc.* **2007**, *129*, 12608–12609.

(13) Yamada, A.; Yamanaka, T.; Hamada, T.; Hase, M.; Yoshikawa, K.; Baigl, D. *Langmuir* **2006**, *22*, 9824–9828.

(14) Madou, M. J. *Fundamentals of Microfabrication*; CRC Press: Boca Raton, FL, 1991.

(15) Fromherz, P.; Kiessling, V.; Kottig, K.; Zeck, G. *Appl. Phys. A* **1999**, *69*, 571–576.

(16) Purrucker, O.; Hillebrandt, H.; Adlkofer, K.; Tanaka, M. *Electrochim. Acta* **2001**, *47*, 791–798.

(17) Atanasov, V.; Knorr, N.; Duran, R. S.; Ingebrandt, S.; Offenhäusser, A.; Knoll, W.; Köper, I. *Biophys. J.* **2005**, *89*, 1780–1788.

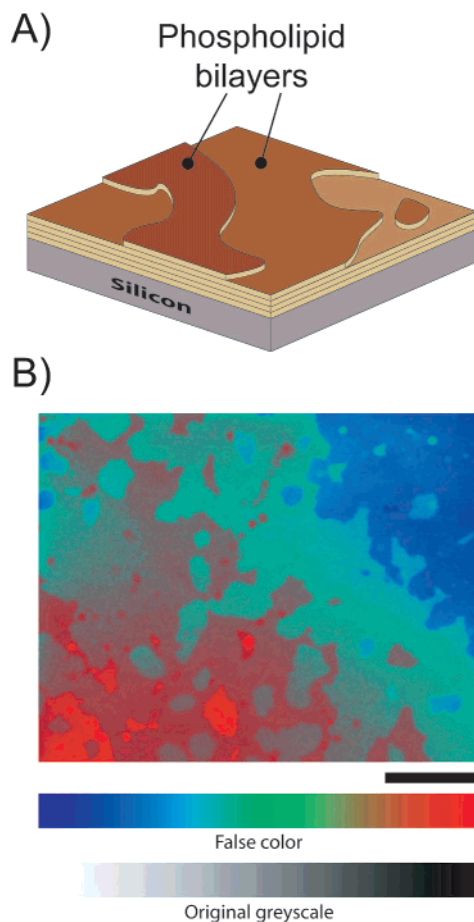


**Figure 2.** (A) Schematic representation of a phospholipid film organized in a multilayered fashion on the silicon substrate. (B) Typical reflection microscopy image of an EPC phospholipid film on silicon. For better visibility, the original grayscale image was automatically converted into false colors. The lighter areas correspond to thinner parts of the film (blue in false color), whereas the darker areas correspond to thicker zones (red in false color). The bars indicate the grayscale/color correspondence that was applied for the image treatment.

containing 0.1 M sucrose and 4.6 mM  $\text{NaN}_3$  in water was introduced between the two electrodes. Electroformation was performed using a sinusoidal AC field (2 V and 10 Hz) for 10 h. The vesicle suspension was then extracted under low shear stress and directly observed by optical microscopy (Figure 3A) or mixed with 2 volumes of 0.1 M glucose solution containing 4.6 mM  $\text{NaN}_3$  previously adjusted to have the same osmolarity as that of the sucrose solution (104 mOsm). The vesicles mixed with the glucose solution were then collected by gravity on a microscope glass slide after 4 h of decantation and observed by optical microscopy (Figures 3B, 5, 6C, and 7C).

**Contact Angle Measurement.** Contact angles of water droplets (Figure 4A) were measured by a tangential method using image J software from side view images of the droplets taken with a CCD camera (PL-A741, Pixellink) mounted on a purpose-built optical setup. For each substrate, the measurements were made in 10 different locations. The contact angle of the chloroform droplets was measured from interference patterns observed near the contact line using a custom-built image analysis software programmed in Matlab.<sup>18</sup> Images were taken with an upright microscope (Nikon Optiphot) in reflection mode using an Acculase 1420-00 laser diode module (Global Laser Technology) as a light source and a CCD camera (PL-A741, Pixellink) for image acquisition. Thirty measurements were performed on each substrate.

(18) de Gennes, P.-G.; Brochard-Wyart, F.; Quéré, D. *Capillarity and Wetting Phenomena: Drops, Bubbles, Pearls, Waves*; Springer: Berlin, 2004.

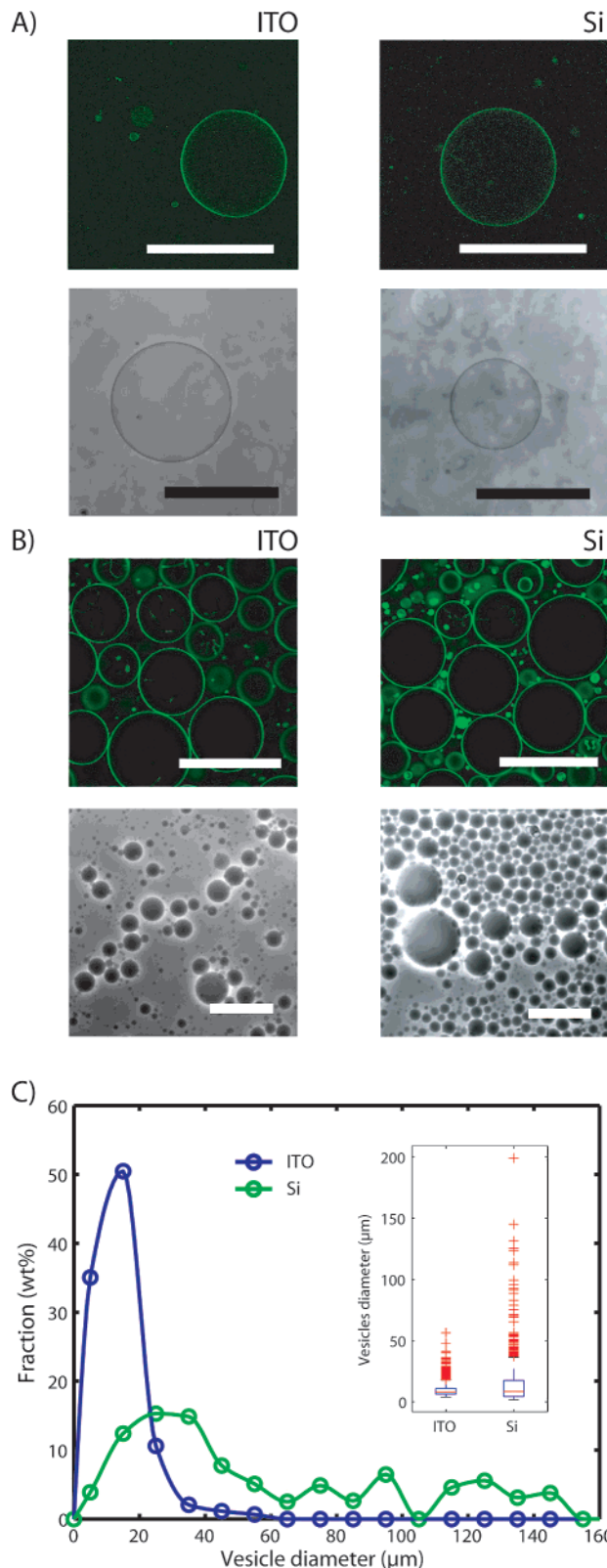


**Figure 3.** Comparison between ITO and Si substrates. (A) Typical confocal fluorescence (top) and phase-contrast (bottom) microscopy images of vesicles in the bulk solution obtained after electroformation on an ITO (left) and Si (right) substrate, respectively. (B) Same as panel A after collection of vesicles by gravity in a glucose solution. (C) Distribution of vesicle sizes in a fraction (wt %) of total phospholipid amount. The inset shows the characteristics of vesicle diameter distributions with box and whisker plots (the horizontal red line, the box, and the red crosses represent the median, the first and third quartiles, and the tails of the distribution, respectively). Scale bars are 100  $\mu\text{m}$ .

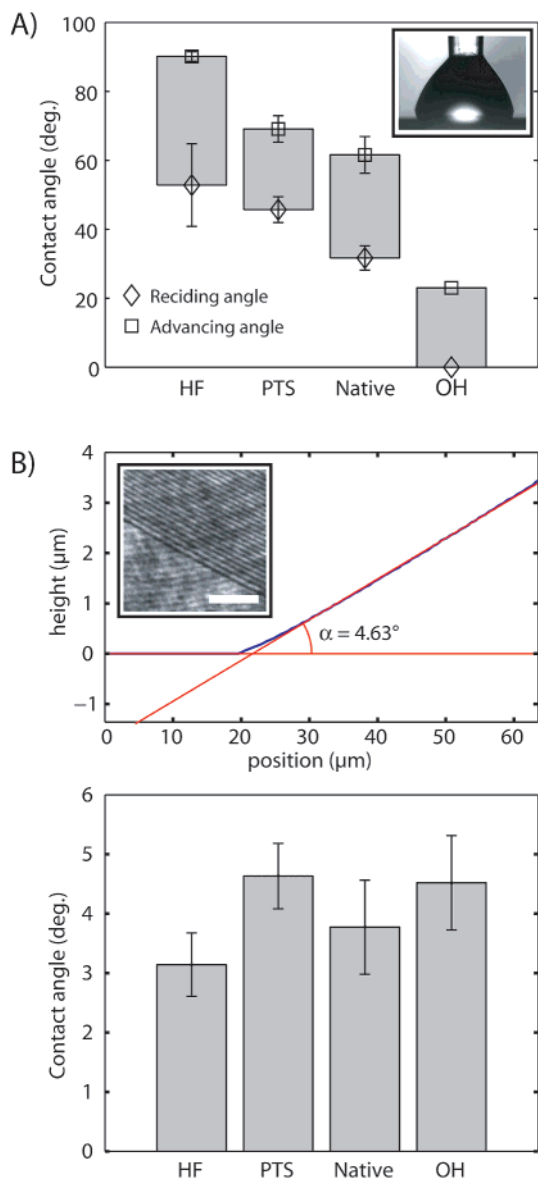


**Figure 4.** (A) Advancing (squares) and receding (diamonds) contact angles of water on Si with various surface chemical treatments: Si made hydrophobic by a hydrofluoric acid treatment (HF), Si with a grafted phenyltrimethoxysilane monolayer (PTS), no treatment (native), and Si treated by air plasma (OH), respectively. For each substrate, the gray area depicts the hysteresis range between advancing and receding contact angles. (B) Receding contact angles of chloroform on Si with various chemical treatments (same as in panel A). Top: typical determination of the contact angle by interferometry. The profile (blue line) of the droplet was calculated from the interference pattern near the contact line (inset, the scale bar is 30  $\mu\text{m}$ ). The linear fit of the profile (red curve) provides the contact angle. Bottom: contact angles measured by interferometry as a function of Si surface treatment. For panels A and B, error bars are  $\pm$ SD.

**Surface Modification.** Si was rendered hydrophilic by air plasma treatment for 2 min at 500 mTorr (Harrick plasma cleaner). Phenyl-modified surfaces were obtained by immersing plasma-activated Si in a 2 vol % solution of phenyltrimethoxysilane in anhydrous toluene containing 1.5 vol % butylamine for 20 min under sonication and rinsing with toluene and water.<sup>19</sup> Si was made hydrophobic by immersion in BOE7:1 for 30 s followed by rinsing with water. The Si microstructures were obtained by photolithography using an AZ5214 photoresist followed by a SF<sub>6</sub> reactive ion dry etching (30

mT, 10 W, 60 s with a Nextral NE100 RIE machine). To make the SiO<sub>2</sub> masks, a 200 nm SiO<sub>2</sub> layer was grown on the silicon wafer (25 min at 1000 °C in wet O<sub>2</sub> atmosphere) followed by photolithography using an AZ5214 photoresist to define the patterns. The thermal oxide layer was then etched by immersion in BOE7:1 for 4 min and rinsed with water. Finally, the photoresist was removed using acetone, and the substrates were sonicated in isopropyl alcohol/acetone for 10 min.

**Microscopy.** Reflection, phase-contrast, and confocal fluorescence microscopy were performed with an Axiovert200 microscope (Zeiss), a DMIL microscope (Leica), and an Axiovert100 microscope equipped with a LSM510 confocal module (Zeiss), respectively. For AFM, we used an NBV 100 microscope (Olympus) equipped with a Nanoscope III controller system operated in tapping mode.

**Image Analysis.** The statistical data from phase-contrast images of vesicles in glucose were collected with custom-built image analysis software based on the Matlab image analysis toolbox. This software automatically extracted the diameters of spherical contrasted objects tested with a least mean squares approximation of sphericity. Each size distribution was established on 5000 measured vesicles (Figures 3C, 5E, 6D, and 7D). Since electroformation is very sensitive to many external parameters (temperature, humidity, etc.), a significant variability can be observed from one experiment to the other. Therefore, for this study, comparisons were always made on one set of experiments performed simultaneously.

## Results and Discussion

**Electroformation on a Silicon Substrate.** Figure 1 shows the experimental setup for electroformation. Briefly, it consists of applying an alternative electric field between one electrode substrate coated with a phospholipid film and an ITO counter-electrode separated by a sucrose solution (swelling solution). Here, we introduce silicon (Si) as the substrate material in contrast to ITO and platinum, which have been mainly used so far. Thanks to the reflective properties of Si, we observed the organization of the dried phospholipid film on the Si surface by using standard microscopy in reflection mode. The constructive and destructive interferences through the film allowed us to observe the thickness variations of the film. Figure 2B shows a typical reflection microscopy image of a phospholipid film on a clean Si wafer without any surface modification. We can clearly observe the stratified organization of the phospholipid film (Figure 2). By AFM, we measured that the average thickness difference between two adjacent zones of different thicknesses was 5–6 nm, which corresponds approximately to one phospholipid bilayer, in agreement with previously reported values.<sup>20–21</sup> The phospholipid is thus organized in a multilayered fashion on the Si substrate. The number of bilayers and average surface area per bilayer depend strongly on the surface chemistry and topology of the Si surface. The different film organizations and the consequences on vesicle formation are presented in the forthcoming sections.

Figure 3 shows the comparison between vesicles obtained with silicon as a substrate to those obtained under exactly the same conditions with ITO as a substrate for the phospholipid film. Confocal microscopy images show that the membranes are similar, regardless of the substrate of the phospholipid film (Figure 3A,B). Since it has been well-established that vesicles produced on ITO by the electroformation method have essentially a unilamellar membrane (i.e., one bilayer),<sup>9</sup> it is expected that vesicles produced on a Si substrate are also unilamellar. It is also interesting to compare ITO and Si substrates with respect to the size distribution of the produced vesicles. Figure 3C shows that, under the same swelling conditions, the distribution of vesicle

(19) Kanan, S. M.; Tze, W. T. Y.; Tripp, C. P. *Langmuir* **2002**, *18*, 6623–6627.

(20) Israelachvili, J. N. *Intermolecular and Surface Force*; Academic Press: San Diego, 1985.

(21) Simonsen, A. C.; Bagatolli, L. A. *Langmuir* **2004**, *20*, 9720–9728.

sizes presents larger median and maximum values in the case of a Si substrate. A possible interpretation could be the better planarity of the crystalline Si surface.

**Effect of Si Surface Chemistry.** Since the surface properties of Si can be easily modified by surface chemistry, we investigated the role of surface properties on vesicle electroformation. Four types of surface treatments were applied to the Si substrates: hydrophilized (OH Si), no treatment (native Si), phenyl-modified (PTS Si), and hydrophobized (HF Si). Hydrophilized Si surfaces were prepared by treating a Si wafer with an air/oxygen plasma, which led to the enrichment of silanol groups at the Si surface.<sup>22</sup> Native Si surfaces correspond to Si wafers and were used as received. Phenyl-modified surfaces were prepared by grafting a self-assembled monolayer of phenyltrimethoxysilane onto the wafer substrate. Hydrophobized Si surfaces were prepared by removing the native oxide layer with hydrofluoric acid. Figure 4 shows the advancing and receding contact angles of water droplets on these substrates. HF Si was the most hydrophobic with a large hysteresis, which is characteristic of inhomogeneous wetting properties or the presence of defects. PTS Si was less hydrophobic than HF Si but more than native Si due to the presence of the phenyl group on the surface. OH Si was the most hydrophilic surface with contact angles below 20°. It is interesting to note that the PTS Si surface had the weakest hysteresis, which indicates a good surface homogeneity after the grafting of the monolayer. Since the phospholipid is dissolved in a chloroform/methanol (9:1 vol/vol) mixture for the film preparation, we measured the contact angle of this solvent on the four different surfaces, which is indicative of the solvophilicity of the surface for this particular solvent (Figure 4B). To this end, we used a method based on interferometry that enabled us to measure the low contact angles.<sup>18</sup> Figure 4B (bottom) shows that the contact angle of chloroform/methanol equals approximately 3–5° for the four surfaces.

The EPC phospholipid film was spread under the same conditions on the four different surfaces and observed by reflection microscopy. On the hydrophilized Si surface (OH Si), large portions of the film dewetted from the solid substrate. This resulted in the formation of portions of a thin film coexisting with thick amorphous parts. In contrast, on the native Si surface, the phospholipid film was well-organized and homogeneously distributed, but small defects on the Si induced the formation of holes in the film. On the PTS Si surface, the film was organized with a homogeneous thickness over a very large surface, almost without any defect. On the hydrophobized surface (HF Si), the phospholipid film was quite thin and did not organize well: the layer looked very inhomogeneous and presented many defects. These differences in the film morphology did not show any correlation to either the hydrophilicity or the solvophilicity properties of the different surfaces (Figure 4A,B). Therefore, we can assume that the interaction between phospholipid molecules and surface is the main control parameter in the phospholipid film organization and not hydrophilicity or solvophilicity. In addition, we noticed that the surface with a large hysteresis (native Si and HF Si) induced many defects in the film, which hampered the smooth organization of the phospholipid molecules. It is thus advantageous to graft a dense monolayer on silicon to improve the film deposition step.

Figure 5 shows the effect of the surface treatment on vesicles obtained after electroformation. In all cases, vesicles were formed, but the size distribution of the resulting vesicles was strongly dependent on the chemical nature of the surface (Figure 5E).

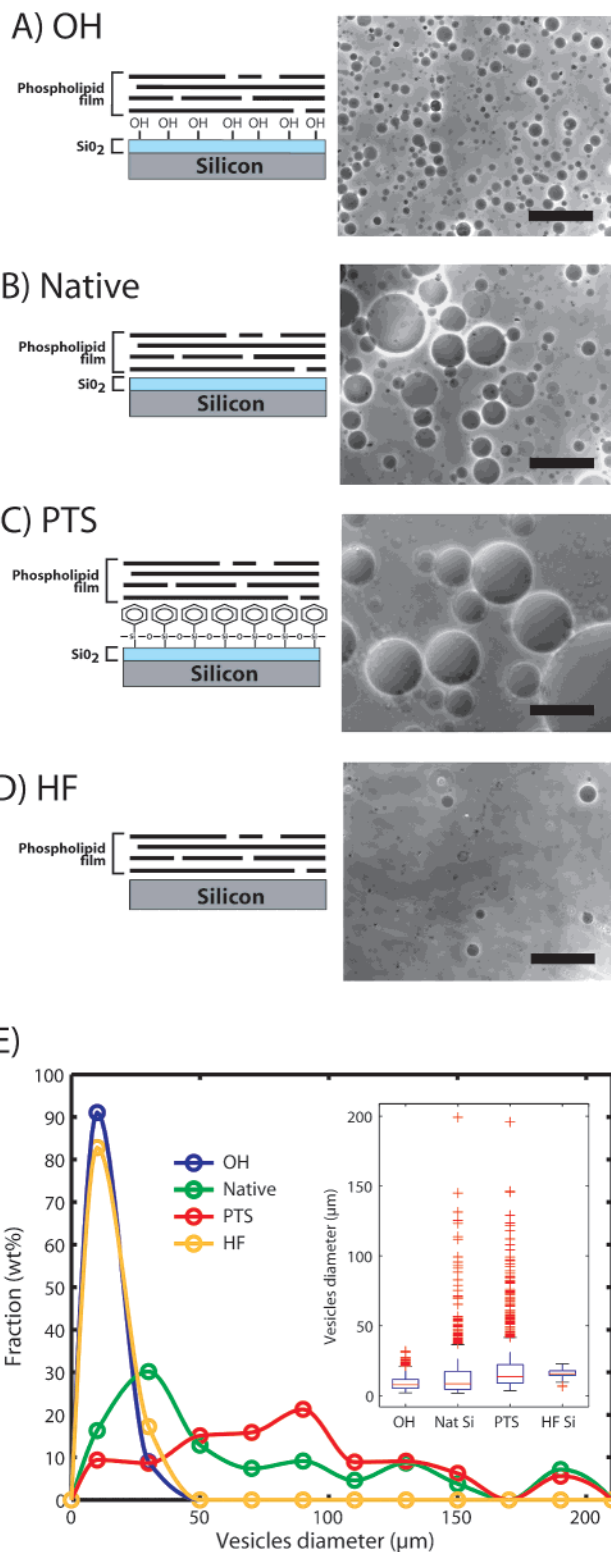


**Figure 5.** Effect of Si surface chemistry on vesicle formation. (A–D) Schematic representations (left) and typical phase-contrast microscopy images (right) of vesicles after electroformation on Si with various surface chemical treatments: Si treated by air plasma (A), no treatment (B), Si with a grafted phenyltrimethoxysilane monolayer (C), and Si made hydrophobic by a hydrofluoric acid treatment (D). Vesicles were collected by gravity in a glucose solution. (E) Distribution of vesicle sizes in a fraction (wt %) of total phospholipid amount. The inset shows the characteristics of vesicle diameter distributions with box and whiskers plots (the horizontal red line, the box, and the red crosses represent the median, the first and third quartiles, and tails of the distribution, respectively). Scale bars are 100 μm.

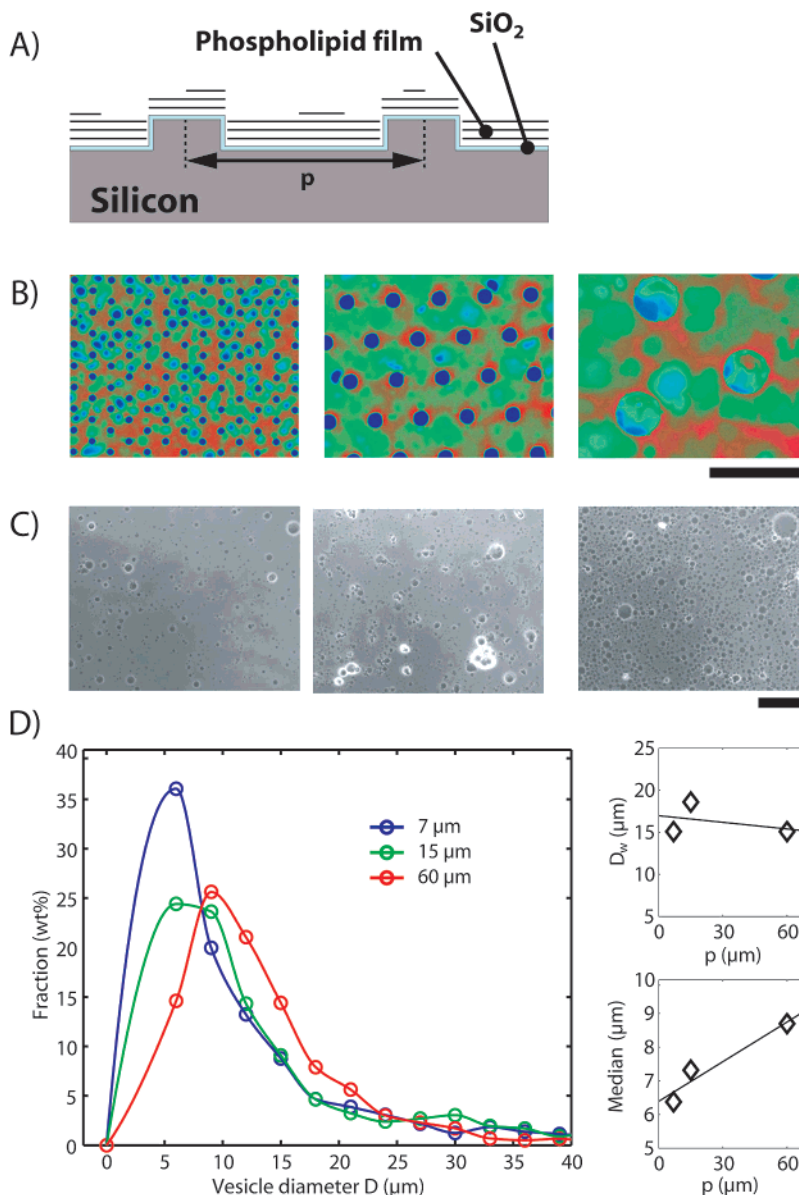


**Figure 6.** Effect of Si surface microstructuring. (A) Schematic representation of the phospholipid film on microstructured Si. The microstructures are hexagonal arrays of micropillars (170 nm high) of various pitch sizes  $p$ . (B) Reflection microscopy images in false colors of the film organization on microstructured Si with a pitch size  $p$  of 7, 15, and 60  $\mu\text{m}$ , respectively. The color treatment is the same as that in Figure 2B. (C) Corresponding phase-contrast images of the vesicles obtained after electroformation. Vesicles were collected by gravity in a glucose solution. (D) Left: distribution of vesicle sizes in fraction (wt %) of total phospholipid amount. Right: mean diameter  $D_w$  (top) and median (bottom) of the distribution as a function of  $p$ . Scale bars are 50  $\mu\text{m}$ .

Vesicles were very small in the case of the hydrophilic surface (Figure 5A), which is probably due to the limited number of bilayers in the organized parts of the phospholipid film. Moreover, the amorphous parts of the film led to the formation of a large amount of small, nonspherical, and multilamellar vesicles. The sizes of vesicles obtained on native Si were typically distributed between 10 and 200  $\mu\text{m}$  (Figure 5B). However, vesicles grown on a PTS Si surface were significantly larger on average than those obtained from native surface (Figure 5C). This can be explained by a better homogeneity of the phospholipid film spread on the modified surface as compared to the native surface, in which the presence of defects affected the organization of the phospholipid film over a large area. In contrast, the swelling on the HF surface (thin film, many defects) gave small vesicles with the lowest yield (Figure 5D).

All these results show that the chemical nature of the surface is essential to the steering of the vesicle formation. Vesicles are larger on chemically homogeneous surfaces (few defects) and

when the nature of the surface is adapted for a good film organization.

**Effect of Si Surface Topology.** To clarify the correlation between phospholipid film organization and vesicle formation, we used the fact that a Si substrate can be easily microstructured to study the effect of a surface micro-/nanostructure on phospholipid film organization and vesicle formation. For this purpose, by using reactive ion dry etching, we prepared a Si substrate with a surface microstructure composed of a network of micropillars with a height of 170 nm (i.e., larger than the typical phospholipid film thickness) and various pitch sizes (7, 15, and 60  $\mu\text{m}$ , respectively). Figure 6B shows typical reflection microscopy images of the phospholipid film spread on the differently microstructured surfaces. As was the case on a native Si surface, the phospholipid film is organized in a stratified way. However, the presence of micropillars clearly affects the phospholipid film organization. While very large areas of uniform thickness were observed on native Si, the phospholipid film was

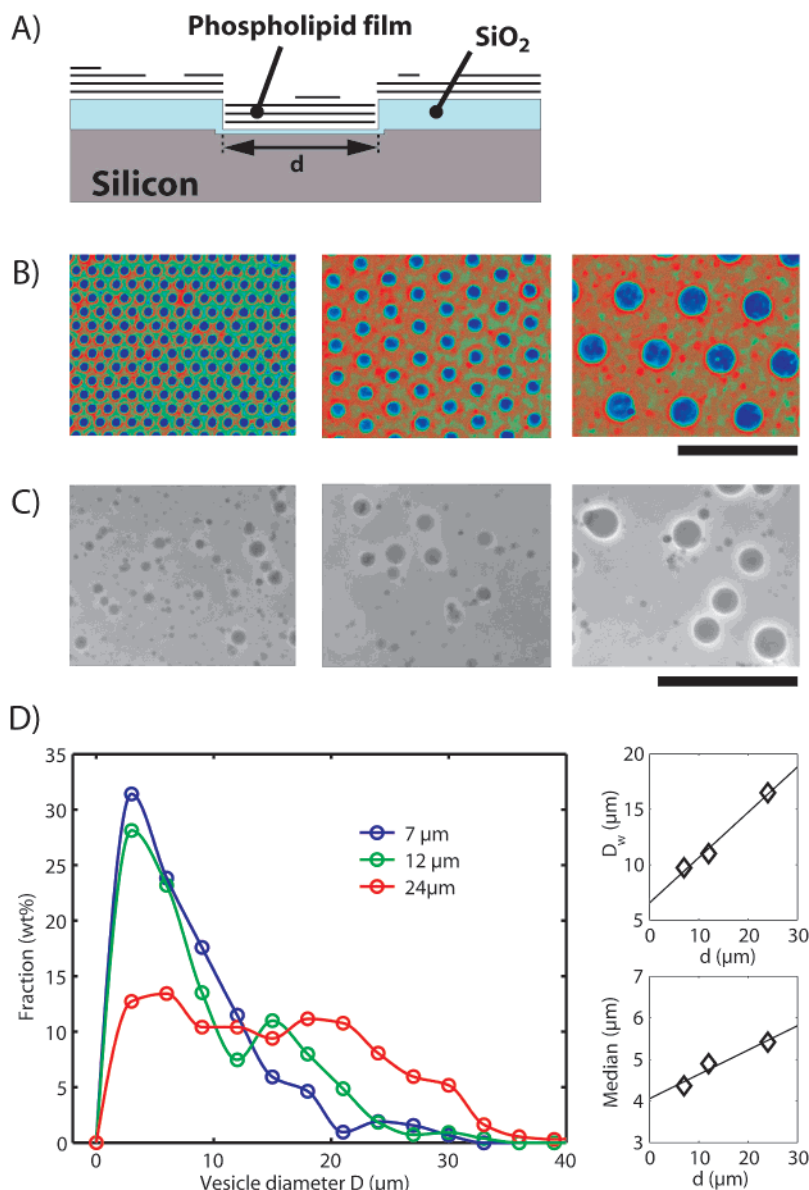


**Figure 7.** Effect of an insulating patterned mask of SiO<sub>2</sub> on the silicon substrate. (A) Schematic representation of the phospholipid film on the substrate. The holes in the silica layer (diameter  $d$ ) are arranged in a hexagonal array. (B) Reflection microscopy images in false colors of the film organization for hole sizes of 7, 12, and 24  $\mu\text{m}$ , respectively. The color treatment is the same as that in Figure 2B. (C) Corresponding phase-contrast images of the vesicles obtained after electroformation. Vesicles were collected by gravity in a glucose solution. (D) Left: distribution of vesicle sizes in fraction (wt %) of total phospholipid amount. Right: mean diameter  $D_w$  (top) and median (bottom) of the distribution as a function of  $d$ . Scale bars are 100  $\mu\text{m}$ .

fragmented due to the presence of the micropillars. The typical size of fragments decreased markedly with a decrease in the pitch size. This shows that a surface microstructure can be used to control the molecular organization of a phospholipid film arranged in a stratified bilayered fashion. Figure 6C,D shows the characteristic phase-contrast microscopy pictures and size distributions of vesicles obtained by the electroformation of phospholipid films spread on the different microstructured Si substrates. There is a clear correlation between microstructure characteristic size (pitch size  $p$ ), phospholipid organization (Figure 6B), and median of the size distribution (Figure 6D). The vesicle size decreases on average with a decrease in  $p$ , which is interpreted as the consequence of the fragmentation of the organized phospholipid film. This assumption is corroborated by the study of Lasic et al. on spontaneous swelling of small and large vesicles on surfaces with various topographies.<sup>23,24</sup> However, the mean

diameter  $D_w$  of vesicles (Figure 6D, top right) is not correlated to the pitch size, which is due to the presence of a small amount of large vesicles for the three kinds of surfaces. Their formation thus involves the swelling of several layers or the fusion of several smaller vesicles. Therefore, it is difficult to precisely control the size distribution of electroswollen vesicles using solely a microstructured electrode.

All these results show that it is possible to fragment the phospholipid film in a controlled way using microstructures. The fragmentation of the film is directly correlated to the size of the electroswollen vesicles, but the presence of vesicles larger than the microstructure characteristic size cannot be avoided.

**Effect of Electric Field Microlocalization.** Finally, we developed a new strategy to obtain better control on the vesicle diameter distribution. In the past few years, there have been

(23) Lasic, D. D. *J. Colloid Interface Sci.* **1988**, *124*, 428–435.

(24) Lasic, D. D.; Belic, A.; Valentincic, T. *J. Am. Chem. Soc.* **1988**, *110*, 970–971.

several attempts to produce monodisperse vesicles by electroformation. The best results have been obtained from phospholipid patterns generated by microcontact printing<sup>25,26</sup> and dry lift-off.<sup>27</sup> Ideally, one vesicle per lipid spot can be obtained with the diameter controlled by the spot size. However, after detachment from the electrode, the collected vesicles usually present a very broad size distribution. Here, we propose to partially insulate the silicon electrode using a 200 nm SiO<sub>2</sub> layer. Circular holes of various diameters (7, 12, and 24  $\mu\text{m}$ , respectively) were etched in the insulating layer to locally expose the silicon to the phospholipid film. The electric field was thus concentrated in the holes where the surface impedance was approximately 60 times lower. Figure 7 shows the film organization and the result of electroformation for the different hole sizes. As in the previous experiments, the film was organized in a stratified fashion, and this led to the formation of vesicles. However, there was a much stronger correlation between the size distribution and the characteristic size of the microstructures. Both mean diameter  $D_w$  and median of the distribution increased significantly with an increase in hole diameter. It is interesting to note that the mean diameter is on the order of the hole diameter. Although the technique will have to be improved to obtain monodisperse

size distributions, to our knowledge, such a control on the size distribution of collected giant vesicles has never been achieved before.

## Conclusion

We described a method for preparing giant phospholipid vesicles in an efficient and controlled way. It consists of the electroformation of vesicles from a phospholipid film spread on a silicon (Si) substrate. By changing the surface properties (chemical composition and microstructures) of Si, it is possible to control both the molecular organization of the phospholipid film and the properties of the final vesicles. Combined with the microlocalization of the electric field, a good control on the size distribution can be achieved. This principle of changing a 2-D surface organization to control a 3-D self-assembly process may find applications in various other self-organized systems.

**Acknowledgment.** We thank G. Velve-Casquillas (LPN CNRS), C. Crozatier (ENS), and M.-A. Guedeau-Boudeville (University Paris 7) for experimental assistance and fruitful discussions. This work was partially supported by ICORP 2006 "Spatio-Temporal Order" project (JST) and CNRS. M.L.B., A.Y., and L.R. were supported by the EADS Foundation, the Japanese Society for Promotion of Science, and Ecole Normale Supérieure, respectively.

LA703391Q

(25) Taylor, P.; Xu, C.; Fletcher, P. D. I.; Paunov, V. N. *Phys. Chem. Chem. Phys.* **2003**, *5*, 4918–4922.

(26) Le Berre, M.; Guedeau-Boudeville, M. A.; Chen, Y.; Baigl, D. *Proc.  $\mu\text{TAS}$*  **2006**, 1399–1401.

(27) Kuribayashi, K.; Takeuchi, S. *Proc.  $\mu\text{TAS}$*  **2005**, 1455–1457.